

# Efficient Raman Sideband Generation in a Coherent Atomic Medium

A.F. Huss, N. Peer, R. Lammegger, E.A. Korsunsky, and L. Windholz  
*Institut für Experimentalphysik, Technische Universität Graz, A-8010 Graz, Austria*  
 (November 23, 2018)

We demonstrate the efficient generation of Raman sidebands in a medium coherently prepared in a dark state by continuous-wave low-intensity laser radiation. Our experiment is performed in sodium vapor excited in  $\Lambda$  configuration on the  $D_1$  line by two laser fields of resonant frequencies  $\omega_1$  and  $\omega_2$ , and probed by a third field  $\omega_3$ . First-order sidebands for frequencies  $\omega_1$ ,  $\omega_2$  and up to the third-order sidebands for frequency  $\omega_3$  are observed. The generation starts at a power as low as 10 microwatt for each input field. Dependencies of the intensities of both input and generated waves on the frequency difference ( $\omega_1 - \omega_2$ ), on the frequency  $\omega_3$  and on the optical density are investigated.

42.50.Gy, 32.80.Qk, 42.50.Hz

## I. INTRODUCTION

Nonlinear optics assisted by electromagnetically induced transparency (EIT) [1] has attracted a great deal of attention in recent years. The effect of EIT is due to creation, via interference of the excitation paths, of a coherent superposition of quantum states which does not participate in the atom-field interaction ("dark" state) [2]. The preparation of atoms in this superposition gives rise to a strongly reduced absorption and refraction of the medium, and at the same time, it may lead to enhancement of the nonlinear optical susceptibility [3]. Therefore, nonlinear optical processes are very efficient in such a coherently prepared medium (which is called sometimes as "phaseonium").

There are several directions in the research of EIT-assisted nonlinear optics which are actively developed at present. One is an efficient nonlinear frequency conversion and generation of coherent electromagnetic radiation unattainable by conventional methods. For example, up-conversion to VUV wavelengths outside the transparency window of most birefringent nonlinear crystals has been experimentally demonstrated with unity photon-conversion efficiency [4,5]; and a high-efficient scheme for generation of c.w. terahertz radiation by use of EIT has been proposed [6]. Another interesting application of the coherent medium concept is a laser frequency modulation by parametric Raman sideband generation, with a total bandwidth extending over the infrared, visible, and ultraviolet spectral regions, and with a possibility of subfemtosecond pulse compression [7,8]. The third very promising direction is based on the fact that the intensity "threshold" for EIT is given by the decay rate of the dark state, which can be made extremely

small if the dark state is a superposition of atomic ground state sublevels. For example, a rate below 40 Hz has been observed in a cell with buffer gas [10], and of order of 1 Hz in a cell with antirelaxation coating [11]. Then, the necessary intensity corresponds to only a few photons per atomic cross section [12–14]. Therefore, one may expect a highly nonlinear response of phaseonium to applied e.m. fields at very low intensity levels, even at a few photon level. The potential of phaseonium has been demonstrated in a recent series of exciting experiments where the group velocity for a light pulse of the order of a few meters per second have been measured [11,15,16]. Such a slow light propagation velocity is an indication of huge optical nonlinearities necessary for strong interactions between very weak optical fields. Recent theoretical work shows that this regime can be used for photon switching [12], for quantum noise correlations [14], for generation of nonclassical states of the e.m. field and atomic ensembles, including entangled states [17–19], and for quantum information processing [18–20].

In the present paper we report on the experimental observation of an EIT-assisted nonlinear optical process which combines the latter two directions: generation of a broad spectrum of Raman sidebands in a medium with small dark state decay rate, hence having a high efficiency even at low input light intensities. The process occurs in an atomic medium interacting with laser radiation in a  $\Lambda$  scheme (Fig. 1).

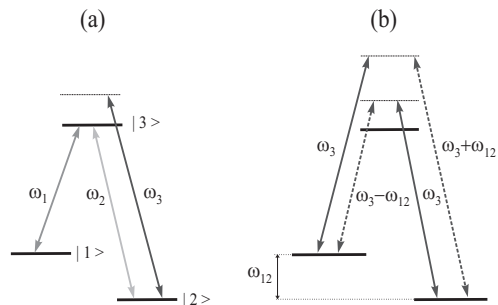


FIG. 1. A system in atoms used in our experiment. (a) The  $\Lambda$ -medium is prepared in the dark state by the resonant pair of fields  $\omega_1$ ,  $\omega_2$  and is probed by the field  $\omega_3$ . (b) Schematic demonstration of the generation of Raman sidebands of the  $\omega_3$  field.

In this system, a pair of laser frequencies  $\omega_1$  and  $\omega_2$  resonantly excites the  $\Lambda$  system (Fig. 1(a)), which leads to creation of a dark superposition of both ground states

|1) and |2) and to the preparation of the atoms in this state via optical pumping. Atoms in the dark superposition act as a local oscillator at frequency  $\omega_{12}$  of the Raman transition. When a third frequency  $\omega_3$  is applied to the system, it will beat against the local oscillator to produce sum and difference frequencies  $\omega_3 \pm n \cdot \omega_{12}$ , i.e., *Raman sideband frequencies* (Fig. 1(b)).  $\omega_3$  may be either of the resonant frequencies ( $\omega_1$  or  $\omega_2$ ) applied off-resonance to the conjugated transition (|2) - |3) or |1) - |3), respectively). Otherwise, it might be derived from an independent laser and tuned either on resonance or off resonance with one of the transitions to some additional upper state (in this case, the interaction scheme is called a double  $\Lambda$  scheme). In our experiment, we have realized these possibilities with all pump waves  $\omega_1$ ,  $\omega_2$  and  $\omega_3$  propagating collinearly, and we have observed the manifold of the Raman sidebands for all three applied frequencies.

One should note that the use of a coherently prepared medium for the efficient generation of Raman sidebands has also been theoretically proposed in Ref. [7], and very recently experimentally realized [8]. In this work, however, the medium (molecular hydrogen and deuterium) is prepared in the dark state by far-off-resonance pulsed radiation, which requires very high intensities. At the same time, the total electromagnetic energy dissipation is very small by virtue of the large detuning from any (molecular) state. Therefore, a very broad spectrum of Raman sidebands can be generated. In our scheme, in opposite, the coherent medium is prepared by resonant low-intensity c.w. radiation. Since in this case the preparation relies on the dissipative process of optical pumping [21], a part of the energy is lost. Nevertheless, the generation is still quite efficient even at very low pump powers. Besides our present work, the generation of a single Raman sideband (Stokes field for frequency  $\omega_1$ ) in coherent medium prepared by low-intensity c.w. field has been observed in Ref. [16] for collinear geometry, and several Raman sidebands have been seen in the related experiment of Ref. [9] on parametric self-oscillation with the counterpropagating driving waves. The aim of the present experiment is to observe the generation of a broad spectrum of Raman sidebands in collinear geometry and to study the dependence of each of them on input laser parameters as well as on the optical density of the medium.

## II. EXPERIMENTAL SETUP

Our  $\Lambda$  system is generated by the excitation of sodium atoms in a vapor cell. The lower states are the two hyperfine levels  $F = 1$  and  $F = 2$ , spaced by  $\omega_{12} = 1771.626$  MHz, of the ground state  $3^2S_{1/2}$ , while the upper state is the hyperfine level  $F' = 2$  of the excited state  $3^2P_{1/2}$ . The vapor cell contains condensed Na and is additionally filled with He as puffer gas at a pressure of 6 torr (at room temperature). It is of cubic form with the

length of 10.3 mm and is made of sapphire to avoid darkening of the cell windows. To compensate stray magnetic fields the Na cell is placed inside an arrangement of three mutually orthogonal Helmholtz coils. For the same reason the heating wires of the cell oven are made of non-magnetic material (Ta) and winded bifilarly. The cell temperature is electronically controlled and stabilized to an absolute accuracy of better than 1 °C. We have performed experiments for temperatures ranging from 100°C to 230°C which corresponds to the saturated Na vapor density from  $3 \cdot 10^9 \text{ cm}^{-3}$  to  $2 \cdot 10^{13} \text{ cm}^{-3}$ . The optical density  $\tau$  has been determined via the absorption of a very weak laser beam tuned on resonance with  $3^2S_{1/2}, F = 2 - 3^2P_{1/2}, F' = 2$  transition: at  $\tau = 1$ , a power of this beam falls by the factor  $1/e$ .

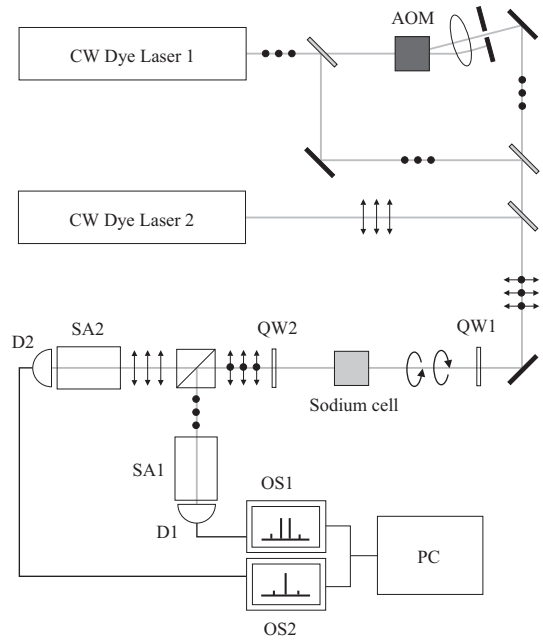


FIG. 2. Scheme of the experimental setup. See description in the text.

The three-frequency radiation is produced by two independent Ar<sup>+</sup>-laser-pumped dye lasers with a linewidth of about 1 MHz (Fig. 2). The first laser system is used to produce EIT in the medium by resonant excitation of the  $\Lambda$ -system  $F = 1 - F = 2 - F' = 2$ . The frequency of this first laser is stabilized to the  $F = 2 - F' = 2$  hyperfine transition of the D<sub>1</sub> line (frequency  $\omega_1$ ) with a frequency accuracy of 2-3 MHz by use of saturation spectroscopy on an external temperature-stabilized Na cell. A part of the beam from this laser, which is linearly vertical polarized, is split off and led through an acousto-optical modulator (AOM) driven by a precise tunable RF-generator at 1700-1800 MHz (resolution of less than 1Hz). The first order sideband produced by the AOM is used as radiation with the frequency  $\omega_2$ . When an AOM modulation frequency of 1771,626 MHz is used, the first order sideband is exactly resonant to the  $F = 1 - F' = 2$  tran-

sition, which corresponds to the Raman resonance necessary for establishment of EIT. A second cw-dye laser system identical to the first one provides the laser beam of frequency  $\omega_3$  with horizontal linear polarization. The frequency  $\omega_3$  can be tuned through the (Doppler broadened with an FWHM of the order of 1 GHz) resonance  $3^2S_{1/2}, F = 2 - 3^2P_{1/2}$  in well defined steps over a range of 32 GHz.

The three laser beams are collinearly overlapped and circularly polarized by a quarter wave plate (QW1). Thus the frequencies  $\omega_1$  and  $\omega_2$  have in the cell the same circular polarization ( $\sigma^+$ ). This polarization configuration was found in our preliminary experiments to produce the best EIT conditions at small intensities. The third frequency  $\omega_3$  is circularly polarized in the opposite direction ( $\sigma^-$ ). The combined light beam has a Gaussian transversal profile with a waist of 0.8 mm, and is almost parallel inside the cell. The input power can be adjusted with a neutral-density filter, and measured before the cell by a photo diode (not shown in Fig. 3). After passing the Na cell, the light is again linear polarized by a second quarter-wave plate (QW2) and the beams of opposite polarizations are separated by use of a polarizing beam-splitter cube (PBS). Each of the beams passes an optical spectrum analyzer (scanning Fabry-Perot interferometer with a free spectral range of 2 GHz, SA1 and SA2) and is detected on separate photo diodes (D1 and D2) connected to a storage oscilloscope (OS1 or OS2). The oscilloscopes are read out by a data acquisition system on a computer (PC). This setup allows us to observe each frequency component, both input and generated ones. The waves  $\omega_1$  and  $\omega_2$  and their generated Raman sidebands (having  $\sigma^+$  polarization in the cell) are detected by the system (SA1, D1, OS1), while  $\omega_3$  and its Raman sidebands (having  $\sigma^-$  polarization in the cell) are detected by the second system (SA2, D2, OS2). We should note that the Raman sidebands have been observed in a setup with all three input frequencies having the same  $\sigma^+$  polarization, too. However, the efficiency was lower because in this case part of the atomic population is optically pumped into the state  $F = 2, m_F = +2$  which is not excited by the applied fields. Moreover, the oscilloscope picture was overcrowded and its analysis was much more complicated.

### III. RESULTS

The first step of our experiments was the measurement of the dark state relaxation rate  $\Gamma$ . For this purpose, the frequency  $\omega_3$  was blocked, and the transmission of frequencies  $\omega_1$  and  $\omega_2$  has been measured as a function of the AOM modulation frequency. The result is a typical EIT transmission peak at 1771,6 MHz, with a halfwidth given by  $\delta_{EIT} = \Gamma + C \cdot I$ , where  $I$  is the total intensity of the frequencies  $\omega_1$  and  $\omega_2$ , and  $C$  is some constant [2]. Thus, the axis offset value of the linear fit to the

measured dependence  $\delta_{EIT}(I)$  can be used as an upper limit for  $\Gamma$ . In this way, we obtained that the value of  $\Gamma$  in our setup is below 3 kHz, which is determined by an AOM frequency jitter and a transit time broadening (due to finite diffusion time of atoms through the beam).

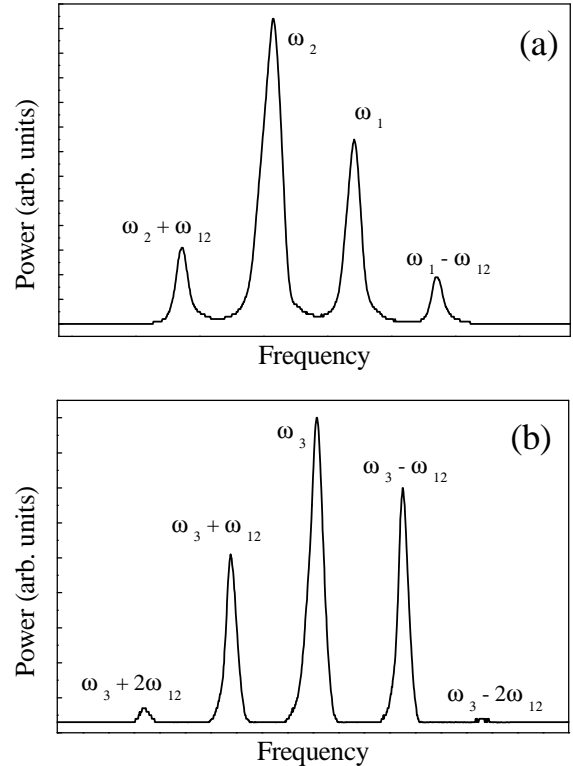


FIG. 3. Typical oscilloscope signal showing the generation of Raman sidebands for all three input frequencies. (a) frequencies with  $\sigma^+$  polarization ( $\omega_1$ ,  $\omega_2$  and their Raman sidebands) detected by SA1, (b) frequencies with  $\sigma^-$  polarization ( $\omega_3$  and its Raman sidebands) detected by SA2.

Fig. 3 shows typical oscilloscope signals demonstrating the generation of Raman sidebands for all three input frequencies. For the frequencies  $\omega_1$  and  $\omega_2$  only the first-order sidebands (Stokes and anti-Stokes fields, respectively) have been observed, while for the field  $\omega_3$  up to the third-order sidebands have been seen, with the higher-order sidebands appearing at larger input power. The intensity of the generated sidebands grows almost linearly with the input power in the range of up to 2 mW for each of the waves  $\omega_1$ ,  $\omega_2$  and  $\omega_3$ . The minimum input power necessary for the generation of the first-order sidebands was found in our experiment to be of the order of 10  $\mu$ W for each wave (the intensity is about 2 mW/cm<sup>2</sup>). We stress that the generation was achieved without the use of buildup cavities. We believe that these results can be considered as an experimental confirmation of the possibility for nonlinear-optical generation processes with a

few photons. With a pulse of a duration of a few  $\mu\text{s}$  (as used, e.g., in experiment Ref. [15]) the intensity of 2  $\text{mW}/\text{cm}^2$  would correspond to the energy of only a few light quanta per atomic cross-section. Thus, one is approaching the regime of nonlinear quantum optics where a large nonlinearity of the medium is created by single photons.

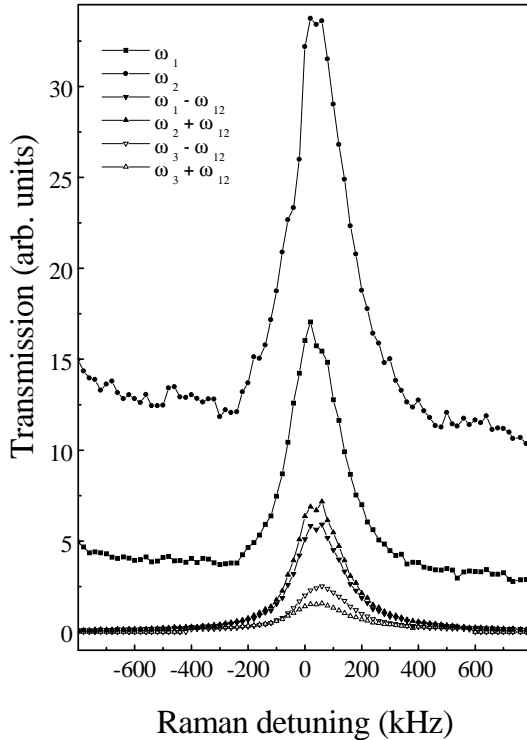


FIG. 4. Dependence of the transmitted light power (plotted on a linear scale) on the Raman detuning  $\delta_R = (\omega_2 - \omega_1) - \omega_{12}$  ( $\omega_{12} = 1771.626$  MHz). Input power  $P_{in} = 700\mu\text{W}$  (intensity  $I = 150$   $\text{mW}/\text{cm}^2$ , equal for each of the input waves  $\omega_1$ ,  $\omega_2$  and  $\omega_3$ ). Temperature of the cell  $190^\circ\text{C}$  ( $\tau = 5.8$ ). The frequency  $\omega_3$  is detuned by 3 GHz above the transition  $3^2S_{1/2}, F = 2 - 3^2P_{1/2}, F' = 2$  and passes the cell nearly unabsorbed.

The nonlinear generation at such low light intensities is already an indirect confirmation of the EIT in action. For a direct confirmation, we measured the dependence of all transmitted frequencies on the AOM modulation frequency (Fig. 4). One can see that the generation of all sideband frequencies occurs only in the narrow range of Raman detuning  $\delta_R = (\omega_2 - \omega_1) - \omega_{12}$ . This is exactly the same range where input frequencies  $\omega_1$  and  $\omega_2$  experience reduced absorption (EIT). The width of the range (10 - 200 kHz depending on the input intensity) is much narrower than the natural width of the excited state  $3^2P_{1/2}$  (10 MHz), and its dependence on the intensity of the frequencies  $\omega_1$  and  $\omega_2$  follows the expected dependence  $\delta_{EIT} = \Gamma + C \cdot I$ . The generation peak is shifted from

exact Raman resonance due to both the buffer gas effects and the a.c. Stark shift [10,22]. The a.c. Stark shift is a differential shift of the ground states  $3^2S_{1/2}, F = 1$  and  $F = 2$  due to the off-resonance coupling to the second excited state  $3^2P_{1/2}, F' = 1$  of the D<sub>1</sub> line (which is 189 MHz apart from the  $3^2P_{1/2}, F' = 2$  state). Our measurements show that this shift is proportional to the *input* intensity of the frequencies  $\omega_1$  and  $\omega_2$  with a slope depending on the optical density; for the parameters of Fig. 4 ( $\tau \approx 6$ ) the slope is about  $0.2$   $\text{kHz}/(\text{mW}/\text{cm}^2)$ . The total absorption of  $\omega_1$  and  $\omega_2$  in Fig. 4 corresponds to 98% outside the EIT transparency window, while at resonance the absorption reduces only moderately to 93%. One must conclude therefore that it is not only reduction of absorption, but also enhancement of the nonlinear susceptibility that assist the generation.

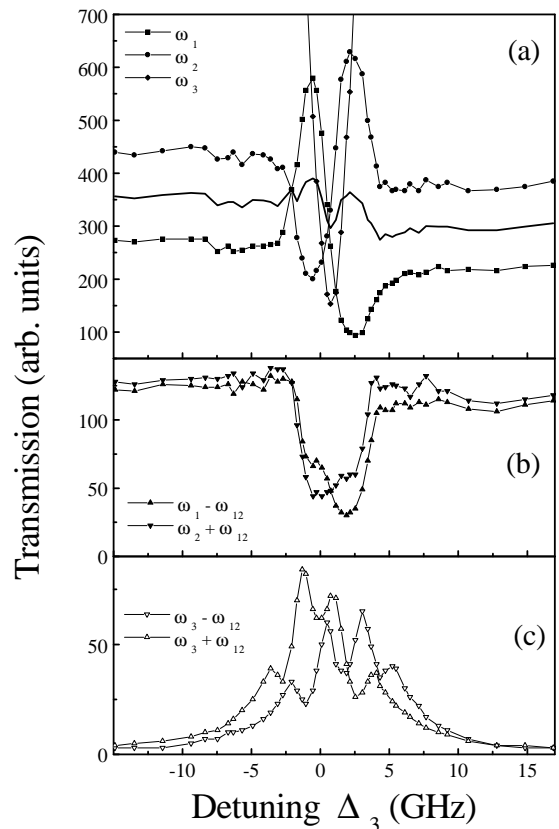


FIG. 5. Dependence of the transmitted light power (plotted on a linear scale) on the detuning  $\Delta_3$  of frequency  $\omega_3$  from the transition  $3^2S_{1/2}, F = 2 - 3^2P_{1/2}, F' = 2$ . (a) For frequencies  $\omega_1$ ,  $\omega_2$  and  $\omega_3$ . The solid curve is the total transmitted intensity of  $\omega_1$  and  $\omega_2$  waves. (b) For the first-order Raman sidebands of frequencies  $\omega_1$  and  $\omega_2$ , (c) for the first-order Raman sidebands of frequency  $\omega_3$ . Input power  $P_{in} = 800\mu\text{W}$  (equal for each of the input waves  $\omega_1$ ,  $\omega_2$  and  $\omega_3$ ). Temperature of the cell  $190^\circ\text{C}$  ( $\tau = 5.8$ ).

The intensity of both generated and transmitted pump fields considerably depends on the value of frequency  $\omega_3$ .

Figure 5 shows the dependence of the intensities on detuning  $\Delta_3$  of the  $\omega_3$  wave from the transition  $3^2S_{1/2}, F = 2 - 3^2P_{1/2}, F' = 2$  in the range of  $\pm 16$  GHz. The  $\omega_3$  wave has almost no influence on transmission of the resonant pump waves  $\omega_1$  and  $\omega_2$  (Fig. 5(a)) and their Raman sidebands (Fig. 5(b)) when  $|\Delta_3|$  is much larger than the Doppler width  $\Delta_D \approx 1$  GHz of the D<sub>1</sub> line. The  $\omega_3$  wave itself is absorbed very weakly in this range (therefore it is not shown in Fig. 5(a)). However, as the resonance with the D<sub>1</sub> line is approached, the  $\Delta_3$  dependence becomes more and more dramatic. Starting from the value  $|\Delta_3|$  of about 8 GHz, one can observe weak intensity oscillations whose amplitude drastically increases for  $\Delta_3$  being in the immediate range of the resonance. When  $\omega_3$  is tuned close to  $3^2S_{1/2}, F = 2 - 3^2P_{1/2}$  ( $\Delta_3 \approx -1.0 \div 0$  GHz), transmission of the  $\omega_2$  wave decreases, while that of the  $\omega_1$  wave increases (Fig. 5(a)). This is because a larger part of atomic population is pumped into the state  $3^2S_{1/2}, F = 1$ . Similar process occurs at  $\omega_3$  being tuned close to  $3^2S_{1/2}, F = 1 - 3^2P_{1/2}$  ( $\Delta_3 \approx 1.7 \div 2.7$  GHz), where transmission of the  $\omega_1$  wave decreases, while that of the  $\omega_2$  wave increases. It is interesting, however, that at these detunings the total transmitted intensity of the  $\omega_1$  and  $\omega_2$  waves (solid curve in Fig. 5(a)) slightly increases over the "transparency level" in the absence of the  $\omega_3$  wave. Despite of this fact, the intensity of generated Stokes ( $\omega_1 - \omega_{12}$ ) and anti-Stokes ( $\omega_2 + \omega_{12}$ ) fields diminishes sharply in the same range of detuning (Fig. 5(b)), so that the total transmitted intensity of  $\omega_1, \omega_2$  and their sidebands remains approximately the same as for very large detunings. This suggests that the absorption is not increased when the  $\omega_3$  field is tuned on resonance, but the nonlinear susceptibility for the Stokes and anti-Stokes fields decreases. At the same time, generation of Raman sidebands of the  $\omega_3$  field is maximized. All these facts indicate that when  $\omega_3$  is close to resonance with the D<sub>1</sub> line, the processes of coherent scattering from each input wave into its Raman sidebands become tightly coupled to one another and start to compete. Thus, the decrease of the  $(\omega_1 - \omega_{12})$  and  $(\omega_2 + \omega_{12})$  fields generation in the range of resonance may be explained by direct competition of this process with the generation of  $(\omega_3 \pm \omega_{12})$  fields. Inside the resonance range, the  $(\omega_1 - \omega_{12})$  and  $(\omega_2 + \omega_{12})$  fields (Fig. 5(b)) reflect the trend of the  $\omega_1$  and  $\omega_2$  fields (Fig. 5(a)), respectively, i.e., increase of the  $\omega_1$  intensity leads to (moderate) increase of the  $(\omega_1 - \omega_{12})$  intensity, etc. On the contrary, the behavior of the  $(\omega_3 \pm \omega_{12})$  sidebands is more complicated: they reveal nice periodical oscillations with detuning  $\Delta_3$ , shifted in phase with respect to each other. These oscillations are apparently related to those observed in [5] and also theoretically predicted in [23] for the generation of  $(\omega_3 + \omega_{12})$  frequency in double  $\Lambda$  atoms, which show a sinusoidal dependence of the generated wave intensity on detuning  $\Delta_3$  and optical density  $\tau$ . So, the shift of the  $(\omega_3 + \omega_{12})$ -wave intensity with respect to the  $(\omega_3 - \omega_{12})$  one may be explained simply by their different detunings from the resonance.

Finally, Fig. 6 demonstrates the measurement results for the optical density dependence of all the waves, both pump and generated ones. The measurements have been performed by taking the oscilloscope pictures at different cell temperatures corresponding to different optical densities. The results presented in Fig. 6 are obtained for the particular case when  $\omega_3$  is tuned exactly on resonance with transition  $3^2S_{1/2}, F = 2 - 3^2P_{1/2}, F' = 1$ . This configuration corresponds to the all-resonant double  $\Lambda$  system, where one expects generation of the  $(\omega_4 = \omega_3 + \omega_{12})$  wave resonant with the  $F = 1 - F' = 1$  transition, and propagation dynamics leading to the matching of the field Rabi frequencies to relation  $g_1/g_2 = g_3/g_4$  [23,24]. However, we have not observed such a matching.

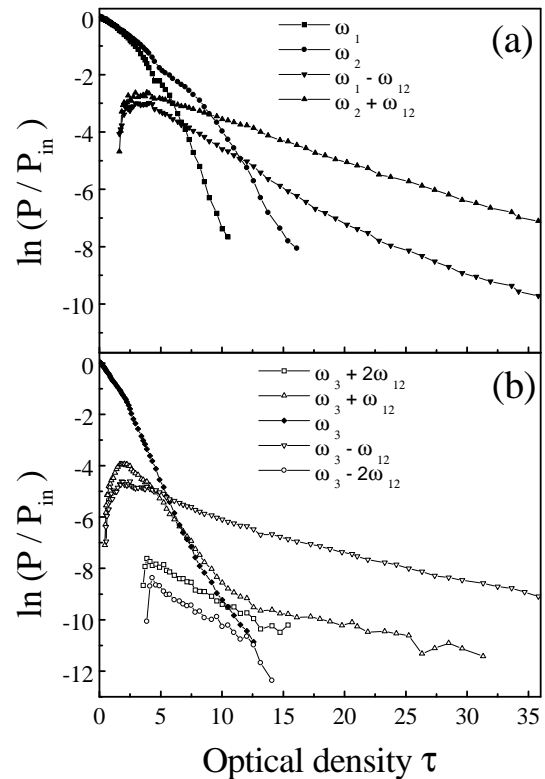


FIG. 6. Optical density dependence of the transmitted light power normalized to the input power  $P_{in} = 450\mu W$  (equal for each of the input waves  $\omega_1, \omega_2$  and  $\omega_3$ ). (a) For frequencies  $\omega_1, \omega_2$  and their Raman sidebands, (b) for frequency  $\omega_3$  and its Raman sidebands. The frequency  $\omega_3$  is tuned exactly on resonance with the transition  $3^2S_{1/2}, F = 2 - 3^2P_{1/2}, F' = 1$ .

One can see from Fig. 6 that power of the pump waves  $\omega_1, \omega_2$  and  $\omega_3$  is attenuated monotonically with the optical density. This attenuation occurs quite fast, with a rate being only slightly lower than that given by Beer's exponential decay. There are at least two reasons for this behavior. First of all, we don't have here real all-resonant

double  $\Lambda$  system since all the waves couple to all possible transitions (which is, in fact, the reason for the broad Raman spectrum generation). Therefore, the energy is transferred not only between the resonant fields, but also goes to the off-resonant Raman sidebands. Second, the preparation of the medium in the dark state relies in our case on optical pumping. In this process, photons from the pump waves  $\omega_1$ ,  $\omega_2$  are absorbed and then rescattered in part spontaneously to bring atomic population in the dark state. The number of spontaneously scattered photons is proportional to the excited state population which is in turn proportional to the light intensity. Therefore, the pump beams experience exponential losses during propagation in the medium. Nevertheless, the atoms are prepared in the coherent superposition of both lower states  $|1\rangle$  and  $|2\rangle$ , and as soon as they are prepared, the generation of the Raman sidebands goes on very efficient. As can be seen from Fig. 6, the first-order sidebands appear already at quite small optical densities ( $\tau = 1 \div 2$ ), grow very fast and reach their maximum at densities of the order of  $\tau = 2.5 \div 5$ . The energy conversion efficiency is approaching the value of 5-7% for the sidebands of  $\omega_1$  and  $\omega_2$  fields, and of 3-4% for the first-order sidebands of  $\omega_3$  field. At this point of maximum generation, the intensity of the first-order sidebands is large enough to induce the generation of the second-order sidebands. Immediately after the initial, very fast, stage of generation, the Raman sidebands start to decay. The resonant sideband ( $\omega_3 + \omega_{12}$ ) is attenuated as fast as the pump waves, while the other Raman sidebands decay slowly due to large detuning from any resonance and, hence, small absorption. It is interesting that different decay rates give rise to a curious situation at larger optical densities when the generated sidebands are more intensive than the pump fields.

#### IV. CONCLUSIONS

In conclusion, we have experimentally demonstrated generation of Raman sidebands in sodium atomic vapor excited on the  $D_1$  line by resonant c.w. optical fields of frequencies  $\omega_1$  and  $\omega_2$ . The first-order sidebands for frequencies  $\omega_1$ ,  $\omega_2$  and up to the third-order sidebands for the probe field of frequency  $\omega_3$  have been observed. The efficient generation takes place due to the preparation of atoms in a dark superposition leading to reduced absorption and enhanced nonlinear susceptibility. This has been directly confirmed by measuring the frequency difference ( $\omega_1 - \omega_2$ ) dependence of the transmission, which evidences that the generation of all sidebands as well as the reduced absorption of pump fields occur only in the narrow range around Raman resonance  $\omega_1 - \omega_2 = \omega_{12}$ . Since the decay rate of the dark state is only a few kHz in our experiment, the generation is efficient even at very low pump powers, with the threshold value being of 10  $\mu W$  for each input wave. Our measurements show that

the Raman sidebands are generated at any value of the frequency  $\omega_3$ . However, the generation of Raman sidebands of the  $\omega_3$  field is maximized and competes with generation of the sidebands of  $\omega_1$  and  $\omega_2$  fields when  $\omega_3$  is close to resonance with the  $D_1$  line. Inside this resonance range, the sideband intensities reveal periodical oscillations with  $\omega_3$ . In the present scheme, the coherent medium is prepared with the c.w. radiation by means of the dissipative process of optical pumping. Therefore, a large part of the radiation energy is lost. This is reflected in the optical density dependence exhibiting fairly fast and almost exponential decay of the resonant pump waves. We believe that much smaller energy losses and, correspondingly, higher conversion efficiency may be achieved by use of the adiabatic passage technique for the preparation of phaseonium [25]. Together with a further reduction of the dark state decay rate (which is certainly possible by using better magnetic field shielding, stabilizing AOM frequency and optimizing the buffer gas pressure), this should allow to readily approach the regime of a few-photon nonlinear optics. Our experimental results also give rise to the challenge of developing a theory of Raman sideband generation by resonant c.w. radiation that will provide an understanding of a complicated interplay of the participating e.m. waves.

This work was supported by the Austrian Science Foundation under project No. P 12894.

- 
- [1] S.E. Harris, *Physics Today* **50**, No. 7, 36 (1997).
  - [2] E. Arimondo, in *Progress in Optics*, ed. E. Wolf (Elsevier, Amsterdam, 1996), vol. 35, p.257.
  - [3] S.E. Harris *et al.*, *Phys. Rev. Lett.* **64**, 1107 (1990).
  - [4] G.Z. Zhang, D.W. Tokaryk, B.P. Stoicheff, and K. Hakuta, *Phys. Rev. A* **56**, 813 (1997); M. Jain, H. Xia, G.Y. Yin, A.J. Merriam, and S.E. Harris, *Phys. Rev. Lett.* **77**, 4326 (1996); A.J. Merriam, S.J. Sharpe, H. Xia, D. Manuszak, G.Y. Yin, and S.E. Harris, *Opt. Lett.* **24**, 625 (1999).
  - [5] A.J. Merriam, S.J. Sharpe, H. Xia, D. Manuszak, G.Y. Yin, and S.E. Harris, *IEEE Journal of Selected Topics in Quantum Electronics* **5**, 1502 (1999).
  - [6] E.A. Korsunsky and D.V. Kosachiov, *J. Opt. Soc. Amer. B* **17**, in press (2000).
  - [7] S.E. Harris and A.V. Sokolov, *Phys. Rev. Lett.* **81**, 2894 (1998); D.D. Yavuz, A.V. Sokolov, and S.E. Harris, *Phys. Rev. Lett.* **84**, 75 (2000).
  - [8] K. Hakuta, M. Suzuki, M. Katsuragawa, and J.Z. Li, *Phys. Rev. Lett.* **79**, 209 (1997); A.V. Sokolov, D.R. Walker, D.D. Yavuz, G.Y. Yin, and S.E. Harris, unpublished; J.Q. Liang, M. Katsuragawa, Fam Le Kien, and K. Hakuta, unpublished.
  - [9] A.S. Zibrov, M.D. Lukin, and M.O. Scully, *Phys. Rev. Lett.* **83**, 4049 (1999).
  - [10] S. Brandt, A. Nagel, R. Wynands, and D. Meschede,

- Phys. Rev. A **56**, R1063 (1997).
- [11] D. Budker, D.F. Kimball, S.M. Rochester, and V.V. Yashchuk, Phys. Rev. Lett. **83**, 1767 (1999).
  - [12] S.E. Harris and Y. Yamamoto, Phys. Rev. Lett. **81**, 3611 (1998).
  - [13] S.E. Harris and L. Hau, Phys. Rev. Lett. **82**, 4611 (1999).
  - [14] M.D. Lukin, A.B. Matsko, M. Fleischhauer, and M.O. Scully, Phys. Rev. Lett. **82**, 1847 (1999).
  - [15] L.V. Hau, S.E. Harris, Z. Dutton, and C.H. Behroozi, Nature **397**, 594 (1999).
  - [16] M.M. Kash et al., Phys. Rev. Lett. **82**, 5229 (1999).
  - [17] G.S. Agarwal, Phys. Rev. Lett. **71**, 1351 (1993).
  - [18] M.D. Lukin and A. Imamoglu, Phys. Rev. Lett. **84**, 1419 (2000).
  - [19] M.D. Lukin, S.F. Yelin, and M. Fleischhauer, Phys. Rev. Lett. **84**, 4232 (2000).
  - [20] M. Fleischhauer and M.D. Lukin, Phys. Rev. Lett. **84**, 5094 (2000).
  - [21] E.A. Korsunsky, W. Maichen, and L. Windholz, Phys. Rev. A **56**, 3908 (1997).
  - [22] A. Nagel, S. Brandt, D. Meschede, and R. Wynands, Europhys. Lett. **48**, 385 (1999).
  - [23] E.A. Korsunsky and D.V. Kosachiov, Phys. Rev. A **60**, 4996 (1999).
  - [24] A.J. Merriam, S.J. Sharpe, M. Shverdin, D. Manuszak, G.Y. Yin, and S.E. Harris, Phys. Rev. Lett. **84**, 5308 (2000).
  - [25] K. Bergmann, H. Theuer, and B.W. Shore, Rev. Mod. Phys. **70**, 1003 (1998).